

## Reply to Referee comment essd-2020-377-RC3

We thank the reviewer for the positive comments and the highlighted issues, which allowed us to improve the final version of the paper and the dataset. Here below a detailed discussion is provided.

### Reply to general comment on the dataset

The file structure will be simplified and a new version of the dataset will be provided. The new FIRMOS dataset will be downloadable as a single file.

### Reply to specific comments

- Line 76: The spectral resolution refers to the sampling resolution  $\Delta\sigma$  of the sinc function, which is  $0.3 \text{ cm}^{-1}$  for FIRMOS (corresponding to  $\text{OPD}_{\text{max}} = 1.66667 \text{ cm}$ ) and  $0.48215 \text{ cm}^{-1}$  for E-AERI (corresponding to  $\text{OPD}_{\text{max}} = 1.03703 \text{ cm}$ ). The instrument line shape (ILS) for E-AERI is corrected to obtain an “ideal” sinc following the procedure outlined in Knuteson et al. 2004, DOI: 10.1175/JTECH-1663.1. The ILS for FIRMOS is characterised a-posteriori with a retrieval procedure and it is approximated by a linear combination of sinc and  $\text{sinc}^2$  (for more details see Bianchini et al. 2019, DOI: 10.5194/amt-12-619-2019), i.e.

$$ILS(\sigma) = \alpha(\sigma) \cdot \text{sinc}\left(\frac{\sigma}{\Delta\sigma}\right) + (1 - \alpha(\sigma)) \cdot \text{sinc}^2\left(\frac{\sigma}{2\Delta\sigma}\right)$$

with

$$\alpha(\sigma) = \text{sinc}\left(\frac{\sigma\Omega}{4\Delta\sigma}\right)$$

where  $\sigma$  is the wavenumber and the parameter  $\Omega$ , fitted in the retrieval procedure, has an average value of  $0.001 \text{ sr}$

The resolution FWHM is approximated  $1.207 \cdot \Delta\sigma$ , i.e. equal to about  $0.36 \text{ cm}^{-1}$  for FIRMOS and  $0.58 \text{ cm}^{-1}$  for E-AERI. All these information will be added in the revised text and the README files

- Line 145: The narrow spectral features in the FIRMOS NESR come from the high-resolution calibration function (the instrument gain function) which contains the absorption features of gasses inside the interferometric path. In the FIR and MIR spectral regions at ground level, water vapour and carbon dioxide absorption inside the instrument has an important contribution. Furthermore, the NESR estimate contains also the noise contribution coming from the measurement of the calibration function, which is performed every 4 sky measurements, and this contribution is comparable with the noise on the sky measurement. The standard deviation estimate is instead the variance of the 4 sky measurements, which are averaged in the final spectrum. It does not contain the noise coming from the calibration function but it contains the effect of possible radiance variations coming from the observed scene. Therefore the standard deviation can be smaller than the NESR estimate when the observed scene is constant. The procedure with which these errors are estimated is described in details in Bianchini and Palchetti 2008, DOI: 10.5194/acp-8-3817-2008.

- Line 154: The frequency scale factor is a constant parameter that can be easily corrected before the application.

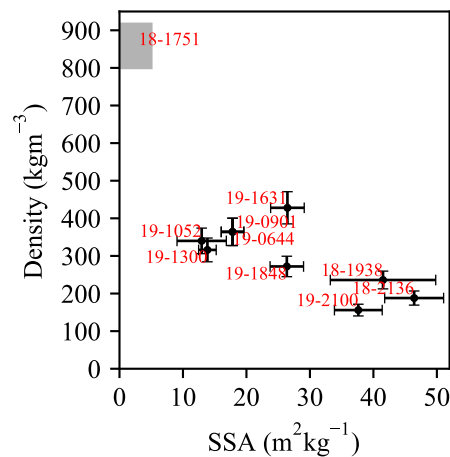
- Line 158: Yes, that's correct, we refer to the FWHM of the applied Norton-Beer strong that is  $0.968 \text{ cm}^{-1}$ .

- Line 160: The a-posteriori bias correction was performed using the residual difference after a fit of the atmospheric state (retrieval analysis) in clear sky conditions and not by a comparison with E-AERI. The comparison with E-AERI was done only for the validation; thus the two measurements are completely independent. The note in the README.firmos will be corrected.

- Line 163: We have made a more accurate estimate of the total error to be applied to the comparison, including all the sources from both instruments, and now the residual differences between the two measurements are only present in a few lines in the 400-450  $\text{cm}^{-1}$  region probably due to slightly different observed scenes because the different FOVs, see also the reply to question 2 of RC1. An improvement of phase error correction algorithm, which might improve the calibration accuracy above 700  $\text{cm}^{-1}$ , will be evaluated in next studies.

- Figure 2, here the spectra are on different sampling grid, thus it is not possible to show the residual difference.

- Figure 5: It will be updated using the figure below



- Table 1: Dates for DUFISSS measurements (18th and 19th February 2019) will be added in Table 1.

- Snow data: We now provide a more comprehensive description of the data in a new README.ssa\_rho as well as contact information if any further questions arise.

The data used in Fig. 5 are written in the file SSA\_rho.csv (for the dots, corresponding to the measured values) and in the file mV\_g.csv for the error bars (qmV and qg columns, 0 denoting a good measurement ( $\pm 10\%$  of the measured value), 1 a medium quality measurement ( $\pm 15\%$ ), and 2 a poor quality measurement ( $\pm 20\%$ )). SSA and density are computed from the raw measurements in mv\_g.csv (with calibrations from calibs.csv), using the retrieval process described in Gallet et al. 2009, DOI: 10.5194/tc-3-167-2009.

Concerning the sample 18-1751, it is an ice sample used as a reference body, but differs from the snow samples: it is a limit case in terms of density (highest possible) and SSA (lowest possible). This is what drove our interest, though it was not possible to characterize its properties as finely as for the snow samples. Indeed, ice density cannot be measured with a snow sampler (the material is too hard). As a matter of fact, we made a rough estimate of the sample density as ice was not the main matter of the snow emissivity study. While pure Ice density is well known ( $917 \text{ kg.m}^{-3}$ ), our sample contained air bubbles lowering its density to an estimated  $850 \text{ kg.m}^{-3}$  (a typical value in the case of glacier ice)  $\pm 15\%$ , which was very conservative. However we agree that this treatment lacked rigour. Reconsidering it, we propose to take a fixed range  $800-917 \text{ kg m}^{-3}$ . Similarly, we couldn't "measure" the SSA of ice with DUFISSS (too hard for the sampler, and too shallow

sample). Such measurement wouldn't make much sense as pure ice is a limit case for the definition of SSA (SSA is defined as the area of air/ice interface per kilogram of snow, in  $\text{m}^2 \text{kg}^{-1}$ , so pure ICE would have an SSA of 0), and for the optical theory behind SSA measurements (Gallet et al., 2009). However, in the shortwave spectrum, pure ice is similar to a snow with an SSA of  $3 \text{ m}^2 \text{ kg}^{-1}$  (Quentin Libois, François Tuzet, personal communication), this is why we put this value in the graph. Finally, we can fix a higher bound for the SSA of glacier ice at  $5 \text{ m}^2 \text{ kg}^{-1}$ , which is a lower boundary for dense snow (see e.g. Fig 10 of Tuzet et al. 2019, DOI: 10.5194/tc-13-2169-2019). We acknowledge the value we used for SSA and the way it was presented in Fig. 5 lacked rigour and might be misleading. We propose to replace the value of  $3 \text{ m}^2 \text{ kg}^{-1}$  by a value range  $0\text{-}5 \text{ m}^2 \text{ kg}^{-1}$  for the SSA of the ice sample, bounded by the value for pure ice ( $0 \text{ m}^2 \text{ kg}^{-1}$ ) and by the lowest measured values for snow ( $5 \text{ m}^2 \text{ kg}^{-1}$ ).

In agreement with these corrections, Fig.5 was updated with a grey box for the ice sample corresponding to the updated bounds. This layout evidences that only a rough estimate of the sample parameters was made.

### **Reply to technical corrections**

All the suggested technical corrections will be accepted